

Natural Vibration and Buckling of General Periodic Lattice Structures

M. S. Anderson*

NASA Langley Research Center, Hampton, Virginia
and

F. W. Williams†

University of Wales Institute of Science and Technology, Cardiff, U.K.

A method is presented for vibration and buckling analysis of arbitrary lattice structures having repetitive geometry in any combination of coordinate directions. The approach is based on exact member theory representing the stiffness of an individual member subject to axial load and, in the case of vibration, undergoing harmonic oscillation. The method is an extension of previous work that was limited to specific geometries. The resulting eigenvalue problem is of the size associated with the repeating element of the structure. A computer program has been developed incorporating the theory, and results are given for vibration of rectangular platforms and a large antenna structure having rotational symmetry. Buckling and vibration results for cable-stiffened rings are also given.

Nomenclature

A_p	= terms in member stiffness matrix
a_p	$= (-1)^{p-1}$
b_p	$= (-1)^p$
c_b	$= r_1/L$
c_j	$= \cos\theta_j$
C	= defined by Eq. (A14)
D_a	= displacement vector of node on axis of rotational symmetry
D_j	= displacement vector of j th repeating element
D_0	= displacement vector of fundamental repeating element
EA	= axial rigidity of a member
EA_T	$= EA_c$ times total number of cables in cable-stiffened ring
EI	= bending rigidity of member
f	= frequency, Hz
H	= depth of truss
j_k	= bay index for j th repeating element in k th coordinate direction
J_0	= number of eigenvalues exceeded if all nodes are clamped
k_{pq}	= submatrices of stiffness matrix of an individual member
K_a	= global stiffness matrix that multiplies D_a , defined by Eq. (A9)
K_j	= global stiffness matrix that couples D_0 and D_j
K_{pq}^j	= global stiffness submatrix for a member connecting D_a and D_j
K_0	= assembled global stiffness matrix that multiplies D_0
K_1	= global stiffness that couples D_a and D_1 , defined by Eq. (A12)
L	= member length
m	= mass per unit length of member
n_k	= index for harmonic response in k th coordinate direction, without subscript refers to θ direction

N_k	= number of bays in k th coordinate direction for which a mode is repetitive
P_0	= compressive force in ring
r	= radial coordinate or ring radius
r_0	= hub radius
r_1	= radial coordinate of node 1
s_b	$= (z_1 - z_a)/L$
s_j	$= \sin\theta_j$
T, T'	= transformation matrices
W	= submatrix contained in T
z_a, z_1	= axial coordinates of nodes a and 1, respectively
θ	= circumferential coordinate
θ_j	= circumferential coordinate of node j
ρ	= radius of gyration
ϕ_j	= defined by Eq. (2)
ω	= circular frequency

Subscripts

c	= cable
p, q	= partitioning of member stiffness matrix or a general integer
r	= ring

Superscripts

H	= Hermitian transpose of a matrix
T	= transpose of a matrix

Introduction

LARGE lattice structures, such as booms, antennas, and platforms proposed for future space applications, have many members and joints that result in very large and expensive analysis problems if the complete structure is modeled in detail. However, these configurations may have only a few different member types and a structural arrangement that has repetitive geometry. The analysis of such structures is greatly facilitated and a considerable saving in computer time is made by using techniques that take advantage of the periodic nature of the structure. Such an analysis for vibration and buckling of a certain class of periodic configurations by Anderson^{1,2} demonstrated that accurate results could be obtained for very large systems with a simple and rapid analysis. The use of exact member theory and an algorithm for determining eigenvalues that assured no modes were omitted were significant factors in achieving accurate results. In the present paper, this analysis has been extended

Presented as Paper 84-0979 at the AIAA/ASME/ASCE/AHS 25th Structures, Structural Dynamics and Materials Conference, Palm Springs, CA, May 14-16, 1984; received Dec. 3, 1984; revision received May 20, 1985. This paper is declared a work of the U.S. Government and therefore is in the public domain.

*Principal Scientist, Structural Dynamics Branch, Structures and Dynamics Division, Associate Fellow AIAA.

†Professor of Civil Engineering, Department of Civil Engineering and Building Technology.

to include any lattice structure having repetitive geometry and loading. The repeating element may have an arbitrary number and arrangement of nodes. For structures having rotational symmetry, there may be nodes along the axis of symmetry that are accounted for in the theory. A description of the theory and results for several example problems are given.

Theory

Equilibrium at the nodes of a repeating element is written in terms of displacements as follows:

$$K_0 D_0 + \sum_j K_j D_j = 0 \quad (1)$$

where K_0 and K_j are transcendental stiffness matrices derived from exact member theory using the exact solution of the linear beam-column equation. These stiffnesses, sometimes referred to as stability functions for buckling problems and dynamic stiffness matrices for vibration problems, are summarized for space frame members by Anderson.^{1,2} The displacement vector D_0 is for all of the nodes of the basic repeating element, and the D_j are the displacement vectors of other repeating elements connected to the basic repeating element. There is no restriction on the number or arrangement of the nodes in the basic repeating element. Because the stiffnesses are based on exact member theory, the effects of member axial load, mass, and frequency are implicitly accounted for in the elements of K_0 and K_j . The key step for the repetitive analysis is to relate D_j to D_0 as follows:

$$\begin{aligned} D_j &= D_0 \exp[2i\pi(n_1 j_1/N_1 + n_2 j_2/N_2 + n_3 j_3/N_3)] \\ &= D_0 \exp(i\phi_j) \end{aligned} \quad (2)$$

where j_k is the number of bays in the k th coordinate direction by which the repeating element must be incremented to reach the j th repeating element, and N_k is the number of bays in the k th coordinate direction for which the mode is repetitive. Note that the structure may be repetitive in any combination of the three coordinate directions and that indexing the repeating element by N_k bays in each coordinate direction generates the complete structure that is analyzed. For ϕ_j , not an integer multiple of π , the stiffness matrix is complex and its eigenvalues correspond to pairs of structural modes. For rotational structures, cylindrical coordinates are used and the structure repeats in the θ direction and could also repeat in the axial direction. To ensure that all possible modes are considered, it is necessary to consider the following integer values of n_k separately:

$$n_k = 0, \pm 1, \pm 2, \dots \pm \text{integer}(N_k/2) \quad (3)$$

It is only necessary to consider combinations of n_k that produce different absolute values of ϕ_j , since changing the sign of ϕ_j only changes the stiffness matrix to its complex conjugate which has the same eigenvalues. Thus, if a structure is repetitive in only one coordinate direction, only positive values of n_k are required. For structures repetitive in two directions, values of n_k need to be taken in the combination $p, \pm q$. However, for many structures having the proper symmetry, the eigenvalue for $p, -q$ will be the same as for $p, +q$. The above theory, which is a generalization of the analysis by Anderson,^{1,2} has been implemented by modifying an existing general space frame buckling and vibration analysis program (BUNVIS) by Banerjee and Williams.³ The program determines vibration frequencies or buckling loads and can include the effects of transverse shear and rotary inertia in individual members. To adapt the program to include repetitive structures, the member stiffnesses K_j that couple one repeating element to another are multiplied by

$\exp(i\phi_j)$ prior to assembly, resulting in a complex Hermitian global stiffness matrix governing D_0 to give

$$KD_0 = 0 \quad (4)$$

In the modified computer program, the matrix K is declared complex and the original coding in BUNVIS for determining eigenvalues is essentially unchanged. A brief description of the eigenvalue analysis used is given in the Appendix. In the case of cylindrical coordinates, the equations correspond to those of MacNeal et al.⁴ or Thomas⁵ for structures having cyclic symmetry, except that in Refs. 4 and 5 conventional finite element stiffness and mass matrices were used rather than stiffness matrices based on exact member theory. MacNeal et al.⁴ developed the real form of the equations and limited their results to connections between adjacent repeating elements only. Thomas⁵ however, pointed out that no additional complexity results from connections to any other repeating element. Many structures having cyclic symmetry also have nodes along the axis that are not repeated. The theory accounting for such cases is given in the Appendix.

Results

The results given by Anderson^{1,2} were primarily for vibration and buckling of simple beam and ring structures where the repeating element has only one node. The present theory and computer program duplicate all of those results exactly. For structures that are repetitive in rectangular coordinate directions, the results for modes that repeat at various wavelengths may not satisfy desired boundary conditions. For such cases, modes with wavelengths that are small compared to the size of the structure may still provide useful information. For example, a buckling load may be associated with a short wavelength mode. If simply supported boundary conditions are desired, the repetitive mode solution satisfies these boundary conditions exactly for many structures and loadings. A very useful application of the theory is to structures having rotational symmetry, where the mode must be repetitive in the θ direction and results are obtained without approximation. Examples of the application of the theory are given in the following sections.

Hexagonal Frame

Belvin⁶ analyzed and performed vibration tests on a number of cable-stiffened frames which have repetitive geometry in the θ direction. Comparison of these results with those from the present method illustrates how all of the eigenvalues of a complete structure can be obtained. The radial rib platform from Belvin⁶ is shown in Fig. 1 and consists of six radial beams emanating from the center and connected at the outer ends by tensioned cables. When the repeating element shown in the upper left-hand corner of Fig. 1 is rotated six times about the central node in increments of 60 deg, the complete hexagonal frame is generated. Vibration modes must be repetitive over six bays so $N_2 = 6$ and, according to Eq. (3), it is necessary to consider harmonics n from 0 to 3 inclusive. The configuration was analyzed as a free-free structure. Several of the lower elastic modes and associated frequencies for in-plane vibration are shown in Fig. 1. The solutions for $n = 1$ and 2 correspond to two independent vibration modes taken as the real and imaginary mode shapes determined from the complex eigenvalue problem. The mode shapes shown are from the present analysis and the beam-dominated modes agree well with those presented by Belvin.⁶ The exact modes were obtained from the deflections of the two nodes used in the repeating element along with Eq. (2) and the solutions of the member differential equations. The complete frame was also analyzed with BUNVIS and the results obtained were identical to those shown in Fig. 1. The finite element results of

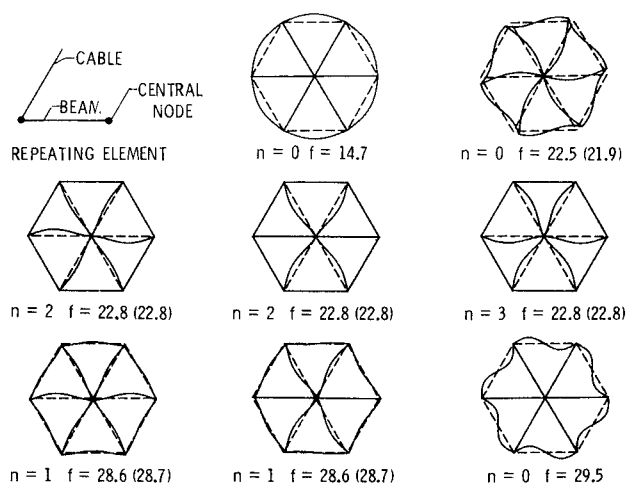


Fig. 1 Vibration modes and frequencies of cable-stiffened hexagonal frame. Values in parentheses from Ref. 6.

Belvin⁶ for the complete configuration used many nodes in each bending member but no interior nodes for the cable, therefore, cable frequencies were not obtained. The only differences in the results of the two analyses for the beam-dominated modes are those for which some observable cable motion is present. For each of the two cable modes shown in Fig. 1, five additional modes were found at the same, or nearly the same, frequency for the harmonics $n=1-3$.

Hexahedral Truss Platform

Vibration of a simply supported rectangular hexahedral truss platform of the type shown in Fig. 2 was considered by Noor et al.⁷ using a continuum and a complete finite element analysis. The truss configuration has members oriented at ± 45 deg and at 0, 90 deg in both surfaces with the pattern repeating in an offset manner. Members with different cross-sectional areas were used in the two surfaces as well as in the core that connects the two surfaces. Because of the symmetry of the configuration, the eigenvalues for the harmonic response n_1, n_2 are the same as those for $n_1, -n_2$. It can be shown that the modes for these two solutions can be combined to satisfy simply supported boundary conditions at intervals of one-half the distance over which the mode is repetitive. Thus, modes that repeat over 16 bays in both directions then give results for a structure simply supported over a span of 8 bays in each direction. Only the eight bays analyzed in the complete model are shown in Fig. 2 along with the nodes that are simply supported. Because the figure was generated from the repeating element, members that may be missing from an edge node do appear at the opposite edge. The complete model has 162 nodes, while only a four-noded repeating element is required in the present analysis as shown in Fig. 2. A comparison of the results from the finite element model (FEM) for the complete structure and the continuum plate model of Ref. 7 with the present theory is given in Table 1. The subscripts on f denote the number of half-waves in each direction for the vibration mode. The analysis gave $f_{pq} = f_{qp}$ as expected for a square symmetric configuration, therefore, only one frequency value is shown. The finite element model used linear stiffness and mass matrices derived by representing each member by a single rod element without bending stiffness. In the repetitive analysis, the bending members used have moments of inertia that give $H/\rho = 30$ for each of the three different area truss members, where H is the depth of the truss and ρ the member radius of gyration. The results for pinned joints were obtained by modifying the stiffness matrix of the individual members by conventional techniques to set all end moments to zero. The comparison is quite good, especially

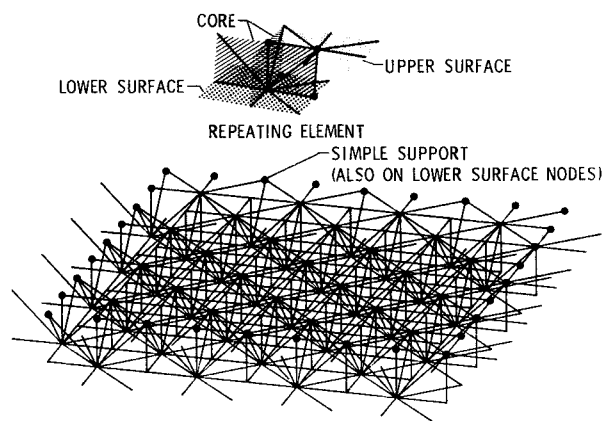


Fig. 2 Simply supported hexahedral truss platform.

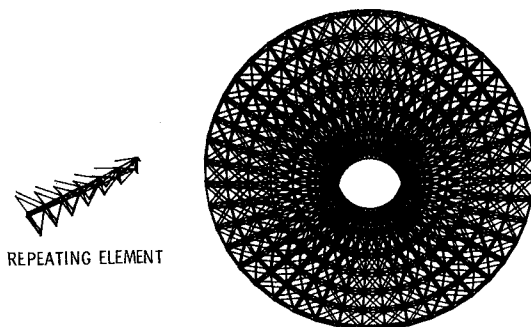
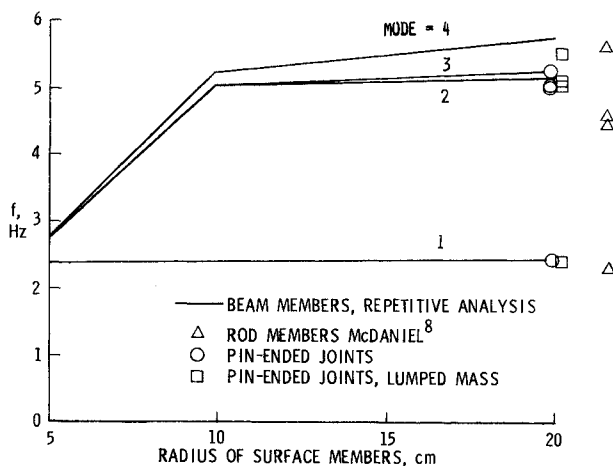
for the lower modes, but there is a tendency for the results from the continuum plate model and the complete model, using the linear eigenvalue analysis, to be high at the higher modes. The pin-ended frequency for the longest member is about 17.8 Hz and the clamped frequency is about 40.3 Hz. The results for pinned joints are in close agreement with the others for the lower modes, but the higher modes are appreciably affected by the nearness of the pin-ended member frequencies. For the rigid joint model, local vibration frequencies are probably near the clamped value, and as a result, there appears to be little effect of local vibration modes on the results for the modes shown. In general, a mode with a zero subscript will not satisfy simply supported boundary conditions. However, the second eigenvalue of the f_{01} mode is given in Table 1 because the displacements were parallel to the truss surfaces, hence, satisfying the simply supported boundary condition.

Antenna Structure

The capability to analyze a complex structure is illustrated by the vibration analysis of the parabolic dish antenna structure shown in Fig. 3 and first analyzed by McDaniel and Chang.⁸ The repeating element has 14 nodes. The original analysis modeled the members as rod elements. The present analysis used tubular members that matched the area of the rod elements by adjusting the radius and thickness of the individual members. The radius-to-thickness ratio of different size members was held constant for each analysis. Several calculations were made for various size members. The first four frequencies are plotted in Fig. 4 as a function of the surface member radius and are compared with previous results. For small radii, the individual members vibrate at frequencies below the frequencies of the antenna modeled with rod elements. As the member radius increases, these modes become sufficiently high that the overall dish modes appear at frequencies about 10% higher than those found previously. There appears to be some discrepancy in the present model as developed from the information provided in Ref. 8 and the actual model analyzed by McDaniel and Chang.⁸ To provide further information on these results, several additional calculations were made using the present theory that should more closely represent the rod elements and lumped mass used in Ref. 8. First, results were obtained for pin joints as shown by the circle symbols which more nearly represent members having axial stiffness only. The present theory accounts for mass exactly. The lumped mass result for pin joints, shown by the square symbols, was obtained by setting the member mass essentially to zero and placing the appropriate concentrated mass at each joint. These results are in significant disagreement with Ref. 8 for the second and third modes. As a final check, an analysis of the complete structure was made using the EAL⁹ computer

Table 1 Frequencies of hexahedral truss calculated from complete and repetitive models

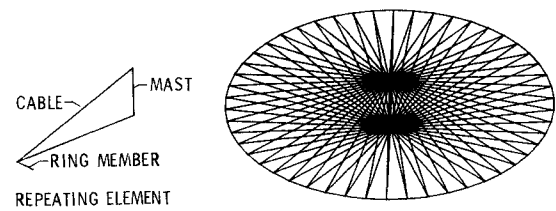
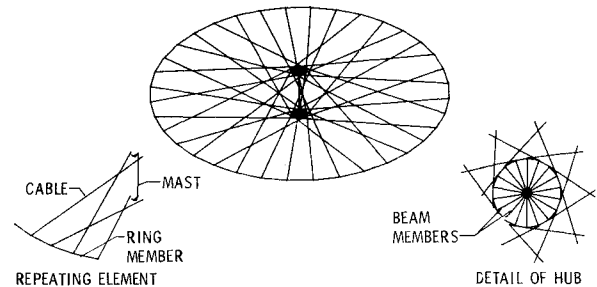
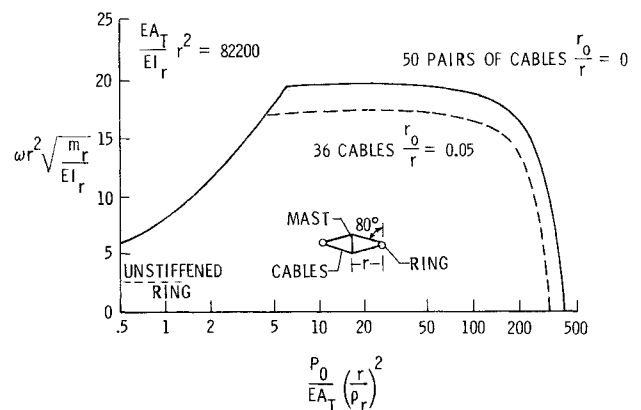
Mode	Frequency, Hz			
	FEM ⁷ truss model	Continuum model ⁷	Present theory	
			Rigid joints	Pinned joints
f_{11}	4.50	4.48	4.57	4.44
f_{12}	7.73	7.67	7.78	7.43
f_{22}	10.08	9.89	10.04	9.44
f_{13}	11.22	11.16	11.15	10.37
f_{01}	12.84	13.09	12.99	12.02
f_{23}	13.06	12.79	12.86	11.74
f_{14}	14.66	14.73	14.42	12.91
f_{33}	15.58	15.15	15.18	13.37
f_{24}	16.18	16.00	15.80	13.79
f_{15}	17.82	18.32	17.60	14.91
f_{34}	18.32	17.94	17.77	14.77

**Fig. 3** 100-m-diam parabolic dish antenna structure.**Fig. 4** Four lowest frequencies of 100-m antenna structure.

program and data derived from Ref. 8. These results were essentially identical to those from the repetitive analysis for the structure with lumped mass and pin joints.

Cable-Stiffened Ring

Buckling and vibration of the cable-stiffened ring shown in Fig. 5 were analyzed by Anderson.^{1,2} However, in that analysis, the attachment at the mast had to be considered clamped, which is correct only for the higher harmonics ($n > 1$, see Appendix). The present analysis can include the mast, but results in an essentially zero torsion frequency in addition to the rigid-body torsion mode for the configuration of Fig. 5. This problem can be eliminated by using cables arranged like bicycle wheel spokes, as shown in Fig. 6. This model demonstrates two of the unique capabilities of the analysis: 1) the ability to connect a member between

**Fig. 5** Cable-stiffened ring.**Fig. 6** Cable-stiffened ring with bicycle-spoke lacing.**Fig. 7** Frequency of cable-stiffened ring as a function of preload.

elements that are not adjacent, and 2) the treatment of a central member. For this case, the θ coordinate at the hub is ± 80 deg from the ring attachment, which provides torsional stiffness to the structure. The hub itself (shown in detail in Fig. 6) is modeled with bending members of the same cross-sectional properties as the ring members. The variation of the lowest frequency with compressive ring force P_0 produced by cable tension is shown in Fig. 7. Nondimensional parameters are used that cause results to be essentially independent of the number of cables. (The definition of all of the parameters used can be found in the nomenclature.) The solid curve is for 50 pairs of centrally directed cables ignoring any zero frequencies. The results for the 36-cable bicycle-wheel lacing are shown as the dashed curve. In the left portion of Fig. 7, cable modes control and the results for both models coincide. At higher loadings, the frequencies of the ring modes for the bicycle arrangement are somewhat lower than for the centrally directed cables. This is attributed to flexibility of the members in the vicinity of the hub. When the lowest frequency goes to zero, the ring buckles. For the bicycle arrangement, the mode has four waves around the circumference as shown in Fig. 8. The radius of the hub was sufficient to drive the torsion frequency above the fundamental frequency shown in Fig. 7. Additional calculations have shown that even a much smaller hub is adequate. In an

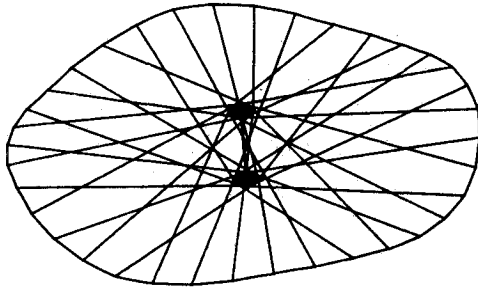


Fig. 8 Buckling mode of cable-stiffened ring with bicycle lacing.

actual design, requirements for torsional stiffness or strength probably would control.

Concluding Remarks

A method is developed to determine, without approximation, vibration or buckling eigenvalues for lattice structures having repetitive geometry and modes that also are repetitive. The method involves nodes of only one repeating element and uses stiffness matrices that are based on exact solutions to the beam-column equations. Thus accurate values can be obtained for all eigenvalues without introduction of nodes between points of connection. A number of methods are available in the literature and implemented in computer programs for structures having cyclic symmetry, i.e., geometry that repeats in the circumferential coordinate. These programs usually use conventional finite elements so that accuracy is lost for higher modes unless an extra number of intermediate nodes are introduced. The authors are not aware of other programs that treat structures that are repetitive in rectangular coordinate directions. If the proper symmetry exists, the present method gives results for such repetitive structures corresponding to boundary conditions of simple support over a length one-half of the length over which the mode is assumed to be repetitive. Such a solution is useful for other boundary conditions if the response wavelengths of interest are small with respect to the size of the structure. For structures having rotational symmetry, such as large antenna configurations proposed for space, the mode must be repetitive around the circumference; thus, the method gives results that are identical to an analysis of the complete structure. Often, such configurations have a central mast connected to all of the repetitive segments. The necessary equations to treat this case are also developed. A computer program has been developed incorporating the repetitive analysis features and results have been obtained for several platform, ring, and antenna configurations. Comparison of these results with previous analyses of the complete structures generally showed good agreement for the lower modes. For higher modes, conventional finite element analysis results tend to be unconservative and, thus, are higher than those obtained using stiffness matrices based on the exact solution of the beam-column equations. For problems having many identical elements, the savings in computer time and storage can be very large compared to methods that analyze the complete structure.

Appendix

Stiffness Matrices When Node Is on Axis of Rotational Symmetry

Consider N identical members which connect a node on the axis of rotational symmetry to nodes which have identical axial coordinates and are uniformly spaced in the θ direction as shown in Fig. A1. In the analysis of the complete structure, that set of members would contribute to the

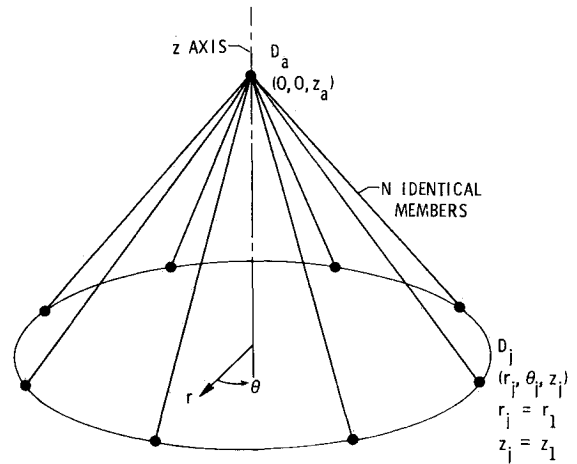


Fig. A1 Central node on z axis connected to several repetitive nodes.

global stiffness matrix as follows:

$$\begin{bmatrix} \Sigma K_{11}^j & K_{12}^1 & K_{12}^2 & \cdots & K_{12}^N \\ K_{21}^1 & K_{22}^1 & 0 & \cdots & \\ K_{21}^2 & 0 & K_{22}^2 & \cdots & \\ \cdots & \cdots & \cdots & \cdots & \\ K_{21}^N & \cdots & \cdots & \cdots & K_{22}^N \end{bmatrix} \begin{bmatrix} D_a \\ D_1 \\ D_2 \\ \vdots \\ D_N \end{bmatrix} \quad (A1)$$

where

$$\Sigma = \sum_{j=1}^N$$

The displacement vector corresponding to each row in Eq. (A1) is also shown. The K_{pq}^j are 6×6 submatrices resulting from transformation of the local member stiffness matrices. For mode shapes that are repetitive in the θ direction, D_j may be related to D_1 as in Eq. (2) by

$$D_j = D_1 \exp[2i\pi n(j-1)/N] \quad (A2)$$

The first row of the matrix of Eq. (A1) times the corresponding displacement vector can then be written as

$$\Sigma \{ K_{11}^j D_a + K_{12}^j D_1 \exp[2i\pi n(j-1)/N] \} \quad (A3)$$

or

$$K_a D_a + K_1 D_1 \quad (A4)$$

The matrices K_a and K_1 can be determined as follows. The member stiffness matrix in local coordinates can be expressed as the four 6×6 submatrices

$$k_{pq} = \begin{bmatrix} A_1 & 0 & 0 & 0 & a_p A_7 & 0 \\ 0 & A_2 & 0 & b_p A_8 & 0 & 0 \\ 0 & 0 & A_3 & 0 & 0 & 0 \\ 0 & b_q A_8 & 0 & A_4 & 0 & 0 \\ a_q A_7 & 0 & 0 & 0 & A_5 & 0 \\ 0 & 0 & 0 & 0 & 0 & A_6 \end{bmatrix} \quad (A5)$$

where

$$a_p = (-1)^{p-1}, \quad b_p = (-1)^p$$

The matrix equation (A5) is written assuming that the nodal displacement vector is given in the order of three displacements followed by three rotations in a right-handed coordinate system and that the member is aligned along the third local coordinate direction. In general, the terms A_p are different for the four submatrices. For a nonvibrating member without axial load, they are equal to the conventional finite element stiffness terms. The member global stiffness matrix can be obtained using the transformation matrices T and T' .

$$T = \begin{bmatrix} W & 0 \\ 0 & W \end{bmatrix} \quad (A6)$$

where

$$W = \begin{bmatrix} s_j & -c_j & 0 \\ c_j s_b & s_j s_b & -c_b \\ c_j c_b & s_j c_b & s_b \end{bmatrix} \quad (A7)$$

and

$$\begin{aligned} c_j &= \cos \theta_j, & c_b &= r_1/L \\ s_j &= \sin \theta_j, & s_b &= (z_1 - z_a)/L \\ \theta_j &= \theta_1 + 2(j-1)\pi/N, & T' &= T|_{\theta_j=0} \end{aligned} \quad (A8)$$

where r_1 , θ_1 , and z_1 are the coordinates of the first repetitive node and z_a is the axial coordinate of the central node. The transformation of Eq. (A7) assumes that one of the principal axes of inertia lies in a meridional plane. The real symmetric matrix K_a can be obtained as

$$K_a = \Sigma K_{11}^i = \Sigma T^T k_{11} T \quad (A9)$$

The nonzero terms in the upper triangle are

$$\begin{aligned} K_a(1,1) &= K_a(2,2) = (A_1 + A_2 s_b^2 + A_3 c_b^2)N/2 \\ K_a(1,5) &= -K_a(2,4) = (A_7 + A_8)s_b N/2 \\ K_a(3,3) &= (A_2 c_b^2 + A_3 s_b^2)N \\ K_a(4,4) &= K_a(5,5) = (A_4 + A_5 s_b^2 + A_6 c_b^2)N/2 \\ K_a(6,6) &= (A_5 c_b^2 + A_6 s_b^2)N \end{aligned} \quad (A10)$$

The terms A_p in Eq. (A10) come from the k_{11} matrix and use has been made of the relations

$$\begin{aligned} \Sigma \cos^2 \theta_j &= \Sigma \sin^2 \theta_j = N/2 \\ \Sigma \cos \theta_j \sin \theta_j &= \Sigma \cos \theta_j = \Sigma \sin \theta_j = 0 \end{aligned} \quad (A11)$$

The matrix K_1 is obtained as

$$\begin{aligned} K_1 &= \Sigma K_{12}^i \exp[2i\pi n(j-1)/N] \\ &= \Sigma T^T k_{12} T' \exp[2i\pi n(j-1)/N] \end{aligned} \quad (A12)$$

The nonzero elements are

$$\begin{aligned} K_1(1,1) &= C(A_2 s_b^2 + A_3 c_b^2), & K_1(1,2) &= -CiA_1 \\ K_1(1,3) &= C(-A_2 + A_3)c_b s_b, & K_1(1,4) &= CiA_7 s_b \end{aligned}$$

$$\begin{aligned} K_1(1,5) &= CA_8 s_b, & K_1(1,6) &= -CiA_7 c_b \\ K_1(3,1) &= (-A_2 + A_3)c_b s_b N \delta_{0n} \\ K_1(3,3) &= (A_2 c_b^2 + A_3 s_b^2)N \delta_{0n} \\ K_1(3,5) &= -A_8 c_b N \delta_{0n}, & K_1(4,1) &= CiA_8 s_b \\ K_1(4,2) &= CA_7 s_b, & K_1(4,3) &= -CiA_8 c_b \\ K_1(4,4) &= C(A_5 s_b^2 + A_6 c_b^2), & K_1(4,5) &= -CiA_4 \\ K_1(4,6) &= C(-A_5 + A_6)c_b s_b, & K_1(6,2) &= -A_7 c_b N \delta_{0n} \\ K_1(6,4) &= (-A_5 + A_6)c_b s_b N \delta_{0n} \\ K_1(6,6) &= (A_5 c_b^2 + A_6 s_b^2)N \delta_{0n} \\ K_1(2,k) &= iK_1(1,k), & K_1(5,k) &= iK_1(4,k) \end{aligned} \quad k=1,2,\dots,6 \quad (A13)$$

where

$$\begin{aligned} C &= (\cos \theta_1 - i \sin \theta_1) \delta_{1n} N/2 \\ \delta_{pq} &= 1, & p &= q \\ &= 0, & p &\neq q \end{aligned} \quad (A14)$$

The terms A_p in Eq. (A13) come from the k_{12} matrix and the following relationships have been used:

$$\begin{aligned} \Sigma \cos \theta_j \exp[2i\pi(j-1)n/N] &= C \\ \Sigma \sin \theta_j \exp[2i\pi(j-1)n/N] &= iC \\ \Sigma \exp[2i\pi(j-1)n/N] &= \delta_{0n} N \end{aligned} \quad (A15)$$

The matrix K_{22}^i is defined as

$$K_{22}^i = (T')^T k_{22} T' \quad (A16)$$

Since T' is not a function of θ_j ,

$$K_{22}^i = K_{22}^1 \quad (A17)$$

If succeeding rows of Eq. (A1) (starting at the second row) are multiplied by $\exp[-2i\pi n(j-1)/N]$ and summed, the result is

$$K_1^H D_a + N K_{22}^1 D_1 \quad (A18)$$

where the superscript H denotes Hermitian transpose. Thus the matrix coefficient of D_1 is the same as that obtained by considering only one member and multiplying the result by N . In the analysis of the complete structure, all stiffness matrices involving members not connected to a central node are multiplied by N to be compatible with Eqs. (A9) and (A12). For members that lie along the axis, the stiffness matrices are generated in the usual way without multiplication by N .

Eigenvalue Analysis

Vibration or buckling eigenvalues are determined in BUNVIS by the theory described by Williams and Wittrick.¹⁰ The theory involves reducing the stiffness matrix for some trial value of the eigenvalue by Gaussian elimination and determining the sign count, which is the number of negative signs on the leading diagonal. The number of eigenvalues exceeded is the sign count plus J_0 , the number of eigenvalues exceeded

by individual members if their ends were clamped. An iterative procedure is used to converge to the desired eigenvalue. The procedure is equally valid for the complex matrix of the repetitive analysis, recognizing that eigenvalues occur in pairs except for the special cases when the matrix is real. These procedures must be modified somewhat to account for a central node. Examination of the matrix K_1 shows that for $n=0$ only the third and sixth rows are nonzero, corresponding to axial displacement and torsion about the axis. For this case the other degrees of freedom are suppressed and only the contribution to J_0 from the axial and torsion modes of members along the axis are counted. For $n=1$, rows 3 and 6 of K_1 are zero. Therefore the corresponding displacements are suppressed. In addition, the contribution to the sign count and J_0 must reflect the fact that the displacement vector is a combination of vectors D_a that are not periodic, and vectors D_j that are periodic around the circumference. This can be accomplished by restricting the motion of all of the nodes along the axis to one plane only (suppressing displacements corresponding to rows 2 and 4 of K_a , for example) and multiplying K_a by one-half. In addition, the stiffness matrix for any member along the axis must be multiplied by one-half. Contributions to J_0 from members along the axis are from bending only and are counted singly (for the theory to apply, the central members must have equal principal moments of inertia and ordinarily the contribution to J_0 for such a member is in multiples of 2). This procedure effectively weights the contribution of the central nodes by one-half compared to other nodes so that final eigenvalues may be considered as occurring in pairs, as for structures without central nodes and having rotational symmetry. For $n>1$, $K_1=0$ and the central node displacements do not couple with exterior node displacements. In this case all degrees of freedom of the central node are suppressed

and no contribution is made to J_0 from a member along the axis.

References

- ¹Anderson, M. S., "Buckling of Periodic Lattice Structures," *AIAA Journal*, Vol. 19, June 1981, pp. 782-788.
- ²Anderson, M. S., "Vibration of Prestressed Periodic Lattice Structures," *AIAA Journal*, Vol. 20, April 1982, pp. 551-555.
- ³Banerjee, J. R. and Williams, F. W., "User's Guide to the Computer Program BUNVIS (BUckling or Natural Vibration of Space Frames)," Dept. of Civil Engineering and Building Technology, The Univ. of Wales Institute of Science and Technology, Cardiff, U.K., Dept. Rept. 5, Feb. 1982.
- ⁴MacNeal, R. H., Harder, R. L., and Mason, J. B., "NASTRAN Cyclic Symmetry Capability," *NASTRAN Users Experience—3rd Colloquium*, NASA TM X-2893, pp. 395-421.
- ⁵Thomas, D. L., "Dynamics of Rotationally Periodic Structures," *International Journal for Numerical Methods in Engineering*, Vol. 14, 1979, pp. 81-102.
- ⁶Belvin, W. K., "Vibration Characteristics of Hexagonal Radial Rib and Hoop Platforms," *Proceedings of the AIAA/ASME/ASCE/AHS 24th Structures, Structural Dynamics and Materials Conference*, Lake Tahoe, NV, Paper 83-0822, May 1983.
- ⁷Noor, A. K., Anderson, M. S., and Greene, W. H., "Continuum Models for Beam- and Platelike Lattice Structures," *AIAA Journal*, Vol. 16, Dec. 1978, pp. 1219-1228.
- ⁸McDaniel, T. J. and Chang, K. J., "Dynamics of Rotationally Periodic Large Space Structures," *Journal of Sound and Vibration*, Vol. 68, No. 3, 1980, pp. 351-368.
- ⁹Whetstone, W. D., "Engineering Analysis Language," *Proceedings of the Second Conference on Computing in Civil Engineering*, American Society of Civil Engineers, New York, 1980, pp. 276-285.
- ¹⁰Williams, F. W. and Wittrick, W. H., "Exact Buckling and Frequency Calculations Surveyed," *Journal of Structural Engineering*, Vol. 109, No. 1, Jan. 1983, pp. 169-187.